Low Temperature Physics | ARTICLE | scitation.org/journal/ltp

Controlled Stochastic Amplification of a Weak Signal in a Superconducting Quantum Interferometer

Cite as: Fiz. Nizk. Temp. **45**, 70–77 (January 2019); doi: 10.1063/1.5082311
Submitted: 20 November 2018

View Online | Export Citation | CrossMark

O. G. Turutanov,[1,a)] V. Yu. Lyakhno,[1] M. E. Pivovar,[2] and V. I. Shnyrkov[3]

AFFILIATIONS

[1] B. I. Verkin Institute for Low Temperature Physics and Engineering, National Academy of Sciences of Ukraine, 47 Nauki Ave., Kharkov, 61103, Ukraine
[2] V.N. Karazin Kharkiv National University 4 Svobody Sq., Kharkov, 61022, Ukraine
[3] Kiev Academic University, 36 Vernadsky Blvd. Kiev, 03142, Ukraine

[a)] **Email:** turutanov@ilt.kharkov.ua

ABSTRACT

In a single-junction niobium superconducting quantum interferometer (RF SQUID loop), a weak low-frequency harmonic signal is amplified when quasi-white Gaussian noise magnetic flux is applied to the loop; such amplification is due to stochastic resonance (SR). We have experimentally shown that if the suboptimal flux noise intensity is insufficient for SR, the mean rate of transitions between the metastable states of the loop, and thus the signal gain, can be controlled by an additional deterministic alternating magnetic flux with frequency being much higher than that of the useful signal to provide the maximal possible gain. The frequency characteristics of a multi-tone composite signal amplification in the cases of controlled stochastic amplification and "pure" SR are compared to each other.

1. INTRODUCTION

Superconductive quantum interference devices (SQUIDs) made from low-and high-temperature superconductors are a key element in the design of the most sensitive magnetometers widely used in laboratory equipment, industrial equipment, biomedical applications, geophysics, etc. The energy sensitivity of SQUIDs, which has reached the quantum-mechanical limit according to the uncertainty principle, worsens in a noisy environment but can be increased[1–6] due to the same thermodynamic fluctuations and external noise using the stochastic resonance (SR) effect. The concept of SR was proposed in the early 1980s.[7,8] SR has various manifestations, the most obvious of which is a non-monotonic increase in a nonlinear system's response to a weak information-carrying (often periodic) signal. As a result, the signal is amplified and reaches its maximum at a certain noise intensity. Other qualitative characteristics of the signal (e.g. signal/noise ratio) also improve at the system output. In order for the SR to be possible in a particular system, the system's residence time in one of its metastable states (MS) must be a function of the noise intensity. The SR effect—both classical and quantum—has been found in many natural and artificial systems. To date, a large number of detailed analytical and experimental studies of SR have been performed.

Criteria have been developed in a variety of approaches for the evaluation of noise-induced ordering.[9,10] In the aperiodic (non-oscillating) systems with strong attenuation (which have been investigated more than others, both theoretically and experimentally), the described phenomenon should be more properly called 'stochastic filtration' (SF) rather than 'stochastic resonance,' as it is commonly called.[11]

Although a significant number of theoretical and model studies of SR in the superconducting loop have been published, few experiments have been dedicated to the investigation of stochastic dynamics in SQUIDs[12] (for example,[1–3]. Therefore, there remain unresolved problems, in this area, including potential practical applications. One such problem is obtaining the maximum signal amplification at a non-optimal and varying noise level.

If the potential barrier height is fixed, the optimal stochastic gain can be achieved by varying the noise intensity[9,10]; however, in most practical cases, the noise intensity may be suboptimal while a change in the device temperature is undesirable. The SR gain coefficient can be controlled by changing the interferometer parameters (primarily, the Josephson junction critical current; the loop inductance hardly changeable) but this will change the 'operation point' of the device which incorporates the interferometer. Therefore, we should look for more convenient mechanisms to control stochastic amplification of the signal in a SQUID at noise below optimum. A number of methods to control stochastic amplification in various systems are proposed, including in SQUIDs, such as suppression of the potential barrier in a single-junction interferometer by a microwave field[13] (later on,[14] this effect was used for parametric amplification of a weak information-carrying signal in a microwave-excited SQUID), dynamic unbalance of the potential symmetry by mixing two harmonics of different amplitudes and initial phase shifts,[15] changing the threshold of the Schmitt trigger utilising the input signal frequency,[16] and by system flip-over in a certain time with a pulse signal,[17] etc. Let us note the theoretical study,[18] which proposes an approach to controlling SR similar to the one we have implemented experimentally; significant differences outlined below.

In this paper, we present experimental results demonstrating the possibility of controlling the stochastic amplification of a weak signal in an RF SQUID loop by adding a variable magnetic flux with frequency significantly exceeding the frequency of the signal, and with sufficiently large amplitude to ensure an increase in the average frequency of loop transitions between its metastable current (magnetic) states. Previously, we have detected such an effect by numerical modelling of the dynamics of magnetic flux in an RF SQUID loop and termed it 'stochastic-parametric resonance'[19]. Preliminary results of calculations for amplification of the broadband composite (four-tone) signal in a controlled stochastic amplification mode as well as 'pure' stochastic resonance mode have also been provided.

2. DYNAMICS OF AN RF SQUID AND EXPERIMENTAL METHOD

The loop in an RF SQUID is the 'heart' of RF SQUID magnetometers. It is a superconductive contour with inductance L, closed by a Josephson junction with critical current I_c, normal resistance R and volume C (Fig. 1 insert). Assuming a sinusoidal current-phase relation $I_s(\varphi) = I_c \sin\varphi$ for Josephson junction, the potential energy of the RF SQUID, which is the sum of the loop magnetic energy and the Josephson junction's binding energy, can be written in dimensionless units as follows:

$$u(x, x_e) = \frac{(x - x_e)^2}{2} - \frac{\beta_L}{4\pi^2}\cos(2\pi x), \tag{1}$$

where $x = \Phi / \Phi_0$ and $x_e = \Phi_e / \Phi_0$ are dimensionless internal (inside the loop) and external (externally applied) magnetic fluxes, respectively, $\Phi_0 \approx 2.07 \cdot 10^{-15}$ Wb is magnetic flux quantum, $\beta_L = 2\pi L I_c / \Phi_0$ is a dimensionless parameter of nonlinearity; the energy is normalized to $\Phi_0^2/2L$. Parameter β_L defines the number and depth of the local minima of the SQUID's potential energy, the potential becomes two- or multi-well when $\beta_L > 1$.

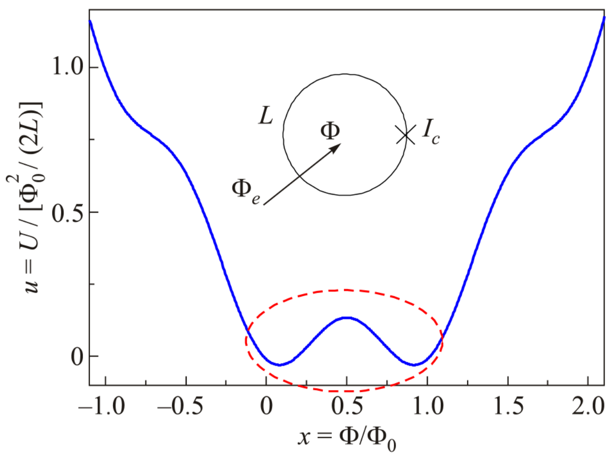

FIG. 1. Normalized potential energy of the superconducting loop with Josephson junction depending on the normalized magnetic flux in the loop. Parameter $\beta_L = 5.3$, the outer constant magnetic flux $x_e = 0.5$. A dashed line denotes a region with two equivalent metastable states. The insert shows a schematic image of the RF SQUID's loop; the parameters shown are explained in the text.

A real device with a loop topology is usually a much more complex node than is schematically shown in Fig. 1. The test interferometer has a self-screened toroidal 3D structure of niobium, with adjustable point contact (Fig. 2) which makes it possible to change the critical current of the contact and β_L during the experiment.

The design of the device is described in detail in.[20] In our experiments, we have investigated interferometers with Josephson junctions of the ScS (superconductor-constriction-superconductor) type at $\beta_L \approx 4.7$–5.4, low impedance ($R \sim 1$ ohm) and relatively small capacitance ($C \approx 3$–200 fF); toroidal coil inductance $L \approx 0.3$ nH. Such a set of parameter values (small C and R) determines the overdamped mode of the SQUID as a stochastic oscillator, which allows us to neglect the second derivative in the flux motion equation[21] and to reduce it to the form convenient for calculations and computer simulations[4–6]:

$$\frac{dx}{dt} = \frac{1}{\tau_L}\left[x_e(t) - x + \frac{\beta_L}{2\pi}\sin(2\pi x)\right], \tag{2}$$

where $\tau_L = L / R$ is the loop flux decay time. As can be seen, this equation describes an aperiodic system. The external flux x_e is the sum of the constant displacement flux ($x_{dc} = 0.5$) symmetrizing the potential, the weak low-frequency signal $x_s = a \sin(2\pi f_s t)$ ($a \ll 1$), uncorrelated white Gaussian noise

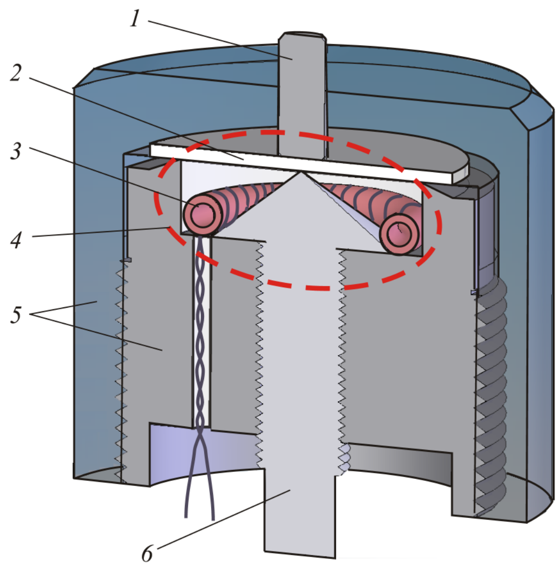

FIG. 2. The toroidal design of the interferometer (sectional view): *1* is a pusher, *2* is a niobic membrane, *3* is a coupling coil, *4* is a quantization boundary, *5* is a body, *6* is an oxidized niobium needle. All parts, except *3*, are made of niobium.

$x_N = \xi(t)$, $\langle\xi(t)\ \xi(t')\rangle = 2D\delta(t - t')$, where D is the noise intensity (variance), and a high-frequency control signal $x_{ctrl} = A \sin(2\pi f_{ctrl}t)$ with $f_{ctrl} \gg f_s$ and the amplitude A, comparable with the mean-square noise deviation $s = D^{1/2}$. Both in the calculations and in the experiments, the noise is quasi-white, its frequency-band is limited by a cut-off frequency f_{cut}. To consider it practically uncorrelated in the context of the discussed SR model, the cut-off frequency should sufficiently exceed the signal frequency, $f_{cut} \gg f_s$. In our calculations and experiments, we selected $f_s = 37$ Hz, $f_{cut} = 50$ kHz and $f_{ctrl} = 50$ kHz. In calculations, the Gaussian quasi-white noise was simulated by a random number generator with a normal distribution and a digital low-pass filter; in the experiment, the Gaussian quasi-white noise was generated by a real physical source (diode) and passed through a low-pass filter.

The experimental setup was similar ideologically to that reported in article.[2] The block diagram of the electrical portion of the experimental setup is shown in Fig. 3.

The alternating magnetic flux is taken to the loop of the test interferometer 1 through the coupling coil L_a in which the current is determined by the sum of voltages from the low-frequency signal generators 3, noise 4, high-frequency control signal 5, and constant displacement source 6. The test interferometer 1 was coupled to an RF SQUID magnetometer 2 which was measuring the resultant flux within the loop 1 via the superconducting magnetic flux transformer L_{tr1} L_{tr2} with coupling coefficient $k = 0.05$. The resistor $r = 0.3$ ohm shunted the transformer, forming a low-pass filter with the cut-off frequency $r / L_{tr} \approx 300$ kHz. It eliminated the influence of the RF (30 MHz) pumping oscillations in the instrumental SQUID oscillatory circuit onto the test interferometer. The spectral density of the magnetic noise flux (sensitivity) of the magnetometer $S_\Phi^{1/2} \approx 2 \cdot 10^{-4}\ \Phi_0 / \mathrm{Hz}^{1/2}$ in the operation frequency band of 2 to 200 Hz. The signal measured by the SQUID magnetometer was fed to one of the double-beam oscilloscopes and the low-frequency spectrum analyzer Bruel&Kjaer type 2033. The number of the instrumentally averaged spectra was 16. Measurements were taken under the control of a personal computer. The coupling coefficients, fluxes, and coil RF currents were determined from the measurements of the amplitude-frequency and the voltage-field (signal) characteristics of the test interferometer while changing the loop flux within $\pm 5\ \Phi_0$. During the setup, the oscilloscope was used in a two-coordinate (X-Y) mode. In the channel of the test interferometer, we used a low-temperature low-noise micro-power amplifier[22] on the HEMT type transistors with the frequency range of 10–100 MHz and adjustable gain 10–80 dB placed inside a superconducting shield near to the SQUIDs.

The cryostat itself with liquid helium (at 4.2 K) was located inside the three-layer permalloy shield. All cryostat inputs were filtered from microwave and RF noise; small-sized batteries were used for the constant displacement and power of the RF amplifiers.

3. RESULTS AND DISCUSSION

Fig. 4 shows a screenshot from the two-beam oscilloscope (see the diagram in Fig. 3) with the oscillograms of the current in coil L_a creating an external input magnetic flux in test interferometer 1 (the top beam), and the resulting magnetic flux in it measured by magnetometer 2 via superconducting transformer L_{tr1}–L_{tr2}. The interferometer demonstrates behavior typical for the scenario of SR (or SF) in a bi-stable system. It can be seen that the input flux represents the sum of the sinusoidal signal and quasi-white noise, and the resulting stream in the interferometer loop is determined by its switching between two nearest magnetic metastable states. Since we did not use the two-state filter (comparator), which gives a telegraph signal on the output, the effect of intrawell oscillations can be seen on the lower oscillogram.

The numerical calculations [1, 2, 4–6] showed that the spectrum density of the internal flux in the SQUID loop at the frequency of the useful signal rapidly rises, peaks and then slowly decreases with the increase of the Gaussian noise intensity D, in accordance with the theory.[9, 10]

Fig. 5 displays the experimentally obtained amplitude spectral density $S_\Phi^{1/2}(f_s)$ of flux Φ inside the interferometer loop at the harmonic signal frequency f_s as a function of mean-square amplitude of the Gaussian noise $D^{1/2}$.

The maximum gain of about 10 dB was obtained in this experiment. It is interesting to note that the exact shape of this 'classical' SR curve turns out to be fairly sensitive to the specific potential relief $U(\Phi)$.

Comparing the calculated and experimental curves, we found that the best fit corresponded to the model of ScS Josephson contact at a finite temperature[23] rather than the

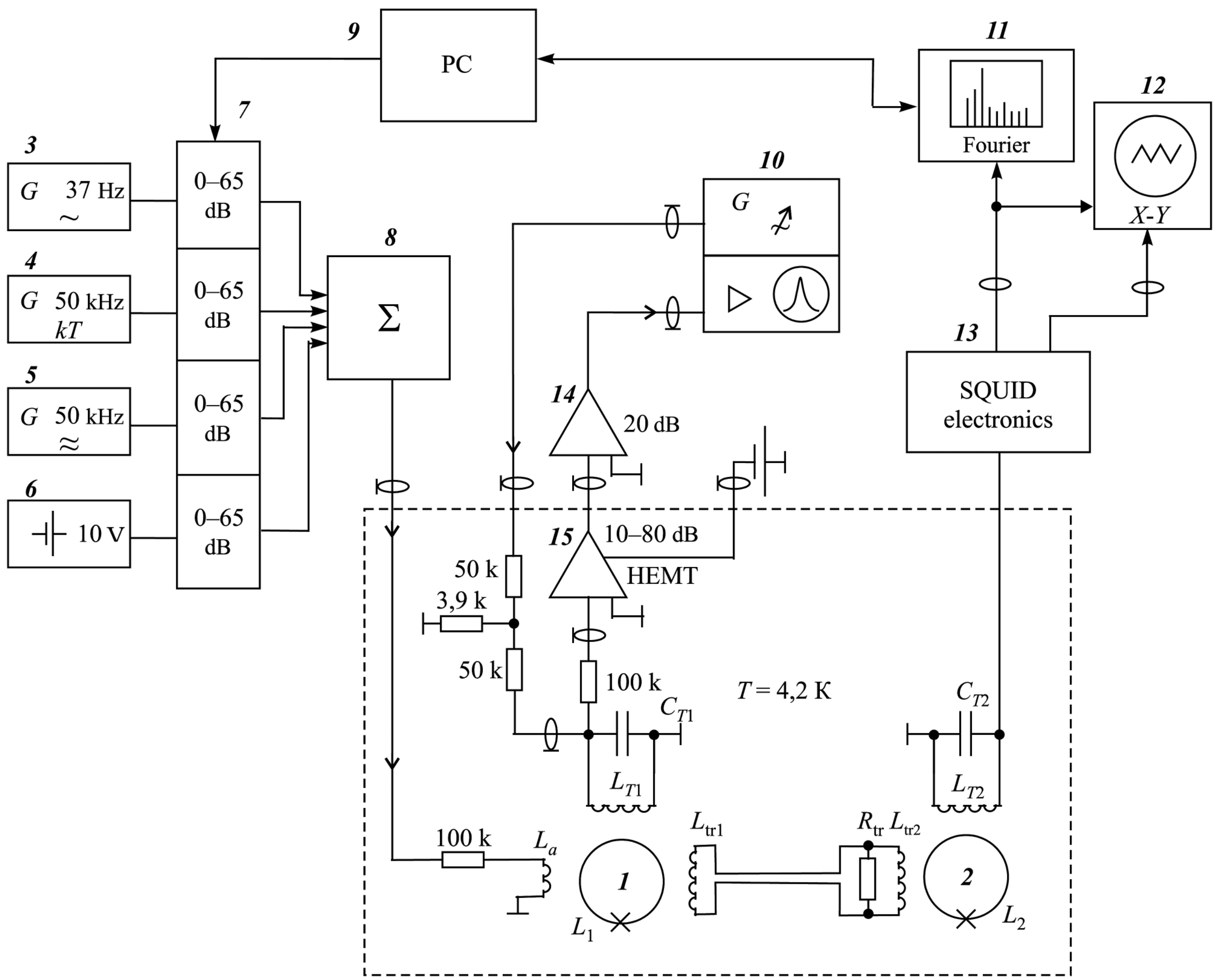

FIG. 3. The block diagram of the electrical part of the experimental setup. The dashed line confines the low-temperature zone of the cryostat with a superconductive shield and a three-layer permalloy shield. Designations *1* is a test loop of the interferometer, *2* is a loop of RF SQUID-magnetometer, *3* is a generator of low-frequency signal G3-34, *4* is a generator of quasi-white noise G2-52, *5* is a generator of high-frequency signal G3-48, *6* is a source of constant displacement, *7* is a block of controlled attenuators, *8* is a signal adder, *9* is a personal computer, *10* is a device for measuring amplitude-frequency characteristics X1–48, *11* is spectrum analyzer Bruel&Kjaer 2033, *12* is oscilloscope C1-83, *13* is RF SQUID electronics, *14* is a 'warm' RF amplifier, *15* is a micro-power cooled HEMT-based RF amplifier. Cryostat input filters are not shown for simplification.

traditionally used tunnel junction model (1). Although the niobium needle is thermally oxidized (6 in Fig. 2) and the critical current calculated from the expression for β_L was small enough ($I_s = 5.2\ \mu A$), the real structure of the point contact may involve both tunnel and direct conductivity in various proportions making difficult to formulate an exact adequate model for its description. The comparison of the experiment with various models is expected to be discussed in detail in future publications.

We showed earlier[19] by a computer simulation that the SR signal gain can be maximized at an insufficient noise level by introducing into the interferometer a controlling high-frequency field which increases the frequency of spontaneous transitions between metastable states up to stochastic synchronization with a useful signal frequency. We called this cooperative effect 'stochastic parametric resonance' (SPR) because the high-frequency field affects the Josephson inductance as a device parameter.

However, many various signal combinations were proposed to control the SR gain (see Introduction) that, one way or another, changed the potential. Particularly, the difference may lie in the auxiliary signal frequency: if it is higher than

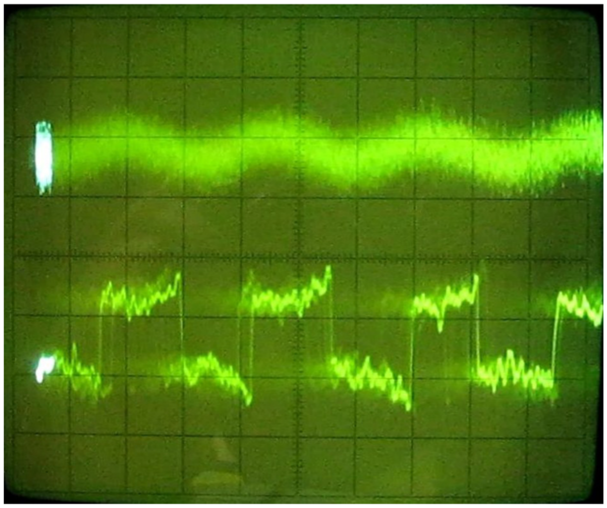

FIG. 4. Oscillograms of the external magnetic flux applied to the interferometer loop (at the top) and measured in the loop of the resulting magnetic flux (at the bottom).

the loop-response decay time R / L, if it is higher than the loop response time L/ R then the signal works much like the temperature, lowering the barrier height.[24] To distinguish the differences between this and other effects as well the SPR discussed here (adiabatic limit, $f_{\text{ctrl}} \ll R / L$), it is probably better to call this effect 'deterministically-assisted stochastic resonance' (DASR). Article[18] discusses theoretical elaboration

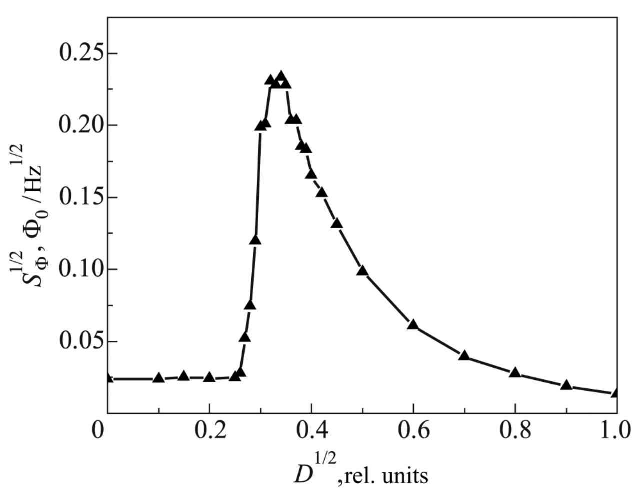

FIG. 5. Experimentally obtained amplitude spectral density $S_\Phi^{1/2}$ (f_s) of the magnetic flux inside RF SQUID loop at the signal frequency f_s as a function of mean-square amplitude of the Gaussian noise $D^{1/2}$. Signal amplitude $a = 0.05$, signal frequency $f_s = 37$ Hz, noise cutoff frequency $f_{cut} = 50$ kHz, nonlinearity parameter $\beta_L = 4.71$, temperature $E = 4.2$ K.

of a similar idea. The authors[18] added an AC field with a frequency only 2–3 times higher than the weak signal frequency and analyzed both commensurate and incommensurate cases. We proposed[19] 'noise substituting' periodic oscillations with a frequency that substantially exceeds the weak signal frequency, $f_{\text{ctrl}} > 10\, f_s$: practically, $f_{\text{ctrl}} \approx 1000\, f_s$.

Fig. 6 shows the experimental curves of the amplitude spectral density $S_\Phi^{1/2}$ (f_s) of the magnetic flux Φ inside the loop at the signal frequency f_s depending on amplitude A of the alternating magnetic flux (control signal) at various noise levels $D^{1/2}$. It can be seen that if the noise intensity is below the optimal value necessary for obtaining maximum stochastic amplification (compare with Fig. 5), then the maximal gain can be reached through additional high-frequency control signal. Since $f_{\text{ctrl}} \gg f_s$, there is no experimental difference between frequency commensurate and incommensurate modes. All the unwanted intermodulation products are far-spaced in the frequency domain and can be easily filtered out.

For the experiment parameters specified under Fig. 6, a generalized dependence can be plotted for normalized amplitude A_n of the control RF field necessary for obtaining maximum amplification $\eta_{\max}$ at a specified (non-optimal) noise level (Fig. 7). The RF field amplitude is normalized to its value $A_{\max}$ corresponding to the maximum amplification in the absence of noise, and the mean-square amplitude of noise s is normalized to its value $s_{\max}$ corresponding to the maximum of SR amplification $\eta_{\max}$ in the absence of the control RF signal (A = 0).

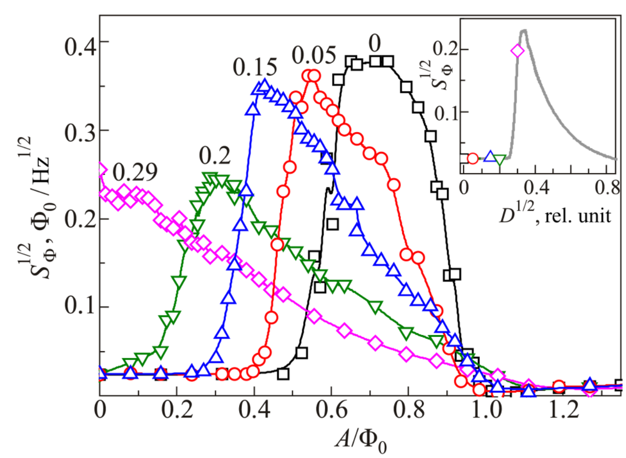

FIG. 6. Experimentally obtained amplitude spectral density $S_\Phi^{1/2}$ (f_s) of the magnetic flux inside RF SQUID loop at the signal frequency f_s as a function of amplitude A of a high-frequency alternating magnetic flux at various non-optimal mean-square amplitudes of the Gaussian noise $D^{1/2}$ (values are near the curves). Signal amplitude $a = 0.05$, signal frequency $f_s = 37$ Hz, noise cutoff frequency $f_{cut} = 50$ kHz, frequency of the control alternating RF flux $f_{ctrl} = 50$ kHz, nonlinearity parameter $\beta_L = 4.71$, temperature $T = 4.2$ K. The insert shows the SR curve with dots at noise intensities $D^{1/2}$ corresponding to the values of the curve parameter in the main figure.

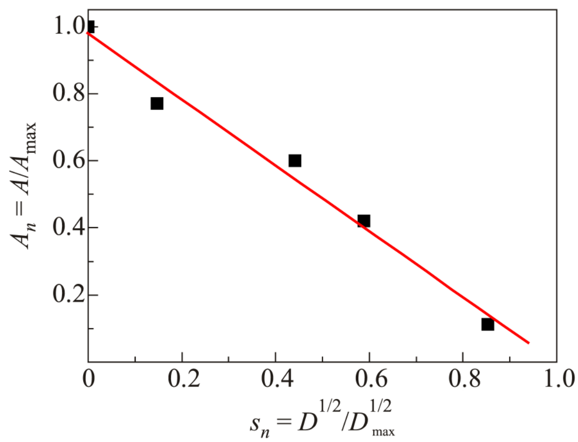

FIG. 7. Normalized amplitude of RF field A_n corresponding to the maximum DASR amplification η_{max} as a function of the normalized noise intensity s_n plotted based on experimental data. The experiment parameters are the same as in Fig. 6.

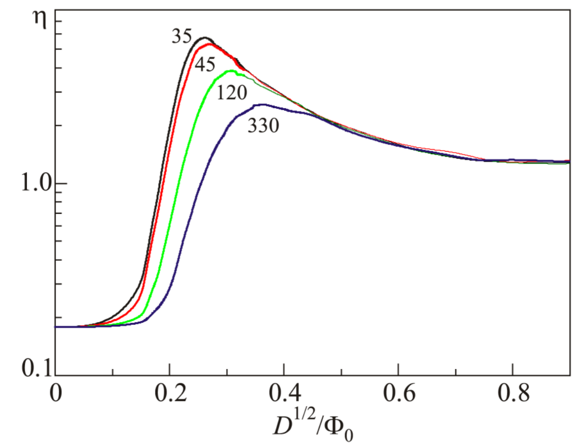

FIG. 8. Stochastic resonance for a signal of complex form: numerical calculation for the dependence of amplification coefficients of four frequency components of the composite signal on noise intensity s. Amplitudes for each of the four harmonic components $a_{1-4} = 0.01\ \Phi_0$, component frequencies in Hz are indicated near the curves, parameter $\beta_L = 5.3$, the cutoff frequency of quasi-white noise $f_{cut} = 50$ kHz, the number of averaged spectra 300.

In the first approximation, this is a close-to-linear dependence. This means certain 'equivalence' and an additivity of noise and high-frequency field as its 'substitute' to obtain the necessary amplification of the weak signal due to the DASR effect. Both factors, acting co-operatively, cause spontaneous transitions between the loop's metastable states. The statement regarding the additivity is valid for the case small signal (linear response). For signals with an amplitude comparable to the barrier height, non-linear effects will appear.

In order to assess frequency characteristics (amplified frequency band, harmonic and intermodulational distortions) during stochastic and stochastic-parametric amplification, we have carried out preliminary model calculation for the signal consisting of the sum of four harmonic components of different frequencies (35, 45, 120, and 330 Hz). The frequencies were selected such as to obtain both low- and high-frequency products of signal mixing for nonlinear amplification arising at large signal amplitude. Let us consider only the case of a small signal (linear response), and the results of non-linear amplification will be will be outlined in other articles. Fig. 8 shows the curves the SR amplification coefficient η for a weak composite signal vs. noise intensity (the values of calculation parameters are provided under the Figure).

Similar curves for the amplification coefficient η vs. amplitude A of the control high-frequency field are calculated for the DASR effect at a fixed suboptimal noise level $D^{1/2} = 0.2\ \Phi_0$ (Fig. 9). It can be seen that, despite the 'equivalence' of noise and control RF signal in terms of obtaining the maximum useful signal gain at a certain frequency (Fig. 6), the bands of amplified frequencies differ (the band becomes narrower for the DASR effect). This can be clearly seen from the comparison of the amplification coefficients of the four harmonic components of the same amplitude, which constitute a complex composite signal, in the effects of SR (Fig. 8) and DASR (Fig. 9).

However, if the amplitude of RF field and noise are normalized (as was done in Fig. 7) separately for each frequency component, then the curves for all frequency components of the signal merge into one demonstrating the universality of the 'law of amplification control' in the DASR effect by RF field

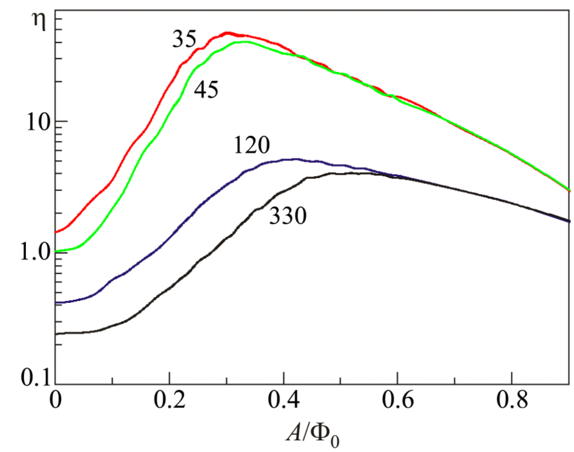

FIG. 9. Stochastic-parametric resonance (DASR) for a signal of complex form: numerical calculation for the dependence of amplification coefficients of four frequency components of the composite signal on the amplitude of the control RF field A at a fixed noise level $D^{1/2} = 0.2\ \Phi_0$, suboptimal. The component frequencies is Hz are indicated near the curves. The frequency of control field $f_{ctrl} = 50$ kHz, all other parameters are the same as in Fig. 8.

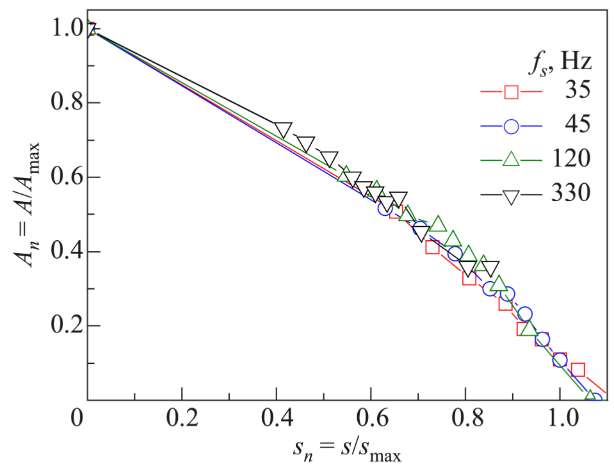

FIG. 10. Universal dependence (in reduced coordinates) of the amplitude of control field A_n necessary for the achievement of maximum amplification $\eta_{\max}$ for the signals with various frequencies, depending on the specified noise level s_n. Each curve is normalized individually. The calculation parameters are the same as in Figs. 8 and 9.

for each specific frequency (Fig. 10), although the absolute values of the gain differ (see Fig. 9).

4. CONCLUSION

In our study, the stochastic resonance effect in a single-junction superconducting quantum interferometer (RF SQUID loop) manifesting itself in an amplification of a weak harmonic low-frequency signal (linear response mode) is experimentally observed. The SR-like effect of a weak signal amplification, that we found earlier by numerical modeling, but caused, unlike SR, by the cooperative action of the noise (stochastic) magnetic flux inside the system and eriodic (deterministic) high-frequency field, is experimentally proved. We suggested designating it as 'deterministically assisted stochastic resonance' (DASR).

A possibility of controlling the stochastic amplification of a weak harmonic signal and maximizing the signal gain at a suboptimal noise level using the DASR effect is experimentally demonstrated. For a weak harmonic signal (linear response mode), the equivalence of the noise effect and the high-frequency control field effect on the amplification coefficient is shown, but the calculation showed that the frequency characteristics of the amplification do differ under controlled (DASR) and 'pure' stochastic (SR) amplification. In addition, the calculation shows that the amplitude of the control RF field at any given suboptimal noise level necessary for obtaining the maximum possible amplification, does not depend on the signal frequency provided that such frequency is much lower than the frequency of RF field and the cutoff frequency of quasi-white noise.

Therefore, due to its universality, DASR effect can be used in the SQUID-based devices, as well as in other devices which have the nonlinearity necessary for SR, for accurate adjustment of stochastic amplification in the environment with a non-optimal and varying noise level. In the latter case, feedback and some adaptive adjustment algorithm should be provided in order to maintain stable amplification. The difference in the frequency characteristics of CP and DASR amplification of weak signals should also be taken into account. For practical application of the described effect, further research should be undertaken, including study of amplification nonlinearity, change of the signal/noise ratio for signals of different amplitude and spectral composition, etc.

REFERENCES

[1]R. Rouse, S. Han, and J. E. Lukens, Appl. Phys. Lett. 66, 108 (1995).
[2]A. D. Hibbs, A. L. Singsaas, E. W. Jacobs, A.R. Bulsara, J. J. Bekkedahl, and F. Moss, J. Appl. Phys. **77**, 2582 (1995).
[3]A. D. Hibbs and B. R. Whitecotton, Appl. Supercond. **6**, 495 (1998).
[4]O. G. Turutanov, A. N. Omelyanchouk, V. I. Shnyrkov, and Yu. P. Bliokh, Physica C 372-376, **237** (2002).
[5]A. M. Glukhov, O. G. Turutanov, V. I. Shnyrkov, A. N. Omelyanchouk, Fiz. Nizk. Temp. **32**, 1477 (2006) [Low Temp. Phys. **32**, 1123 (2006)].
[6]O. G. Turutanov, V.A. Golovanevskiy, V. Yu. Lyakhno, and V. I. Shnyrkov, Physica A **396**, 1 (2014).
[7]R. Benzi, A. Sutera, and A. Vulpiani, J. Phys. A **14**, L453 (1981).
[8]C. Nicolis and G. Nicolis, Tellus 33, 225 (1981).
[9]L. Gammaitoni, P. Hanggi, P. Jung, and F. Marchesoni, Rev. Mod. Phys. **70**, 223 (1998).
[10]V. S. Anischenko, A. B. Neiman, F. Moss, L. Schimansky-Geier, Physics-Uspekhi **169**, 7 (1999) [Phys.-Usp. 42, 7 (1999)].
[11]Yu. L. Klimontovich, Physics-Uspekhi **169**, 39 (1999) [Phys.-Usp. **42**, 37 (1999)].
[12]A. R. Bulsara, Nature **437**, 962 (2005).
[13]V. I. Shnyrkov, V. A. Khlus, and G. M. Tsoi, J. Low Temp.Phys. **39**, 477 (1980).
[14]V. I. Shnyrkov and Yu. P. Bliokh, XII *Trilateral German-Russian-Ukrainian Seminar on High-Temperature Superconductivity*, Program and Abstracts (Kiev, 1999), p. 81.
[15]G. Schmid and P. Hanggi, Physica A **351**, 95 (2005).
[16]L. Gammaitoni, M. Locher, A. Bulsara, P. Hanggi, J. Neff, K. Wiesenfeld, W. Ditto, and M. E. Inchiosa, Phys. Rev. Lett. **82**, 4574 (1999).
[17]J. Mason, J. F. Lindner, J. Neff, W. I. Ditto, A. R. Bulsara, and M. L. Spano, Phys. Lett. A **277**, 13 (2000).
[18]S. Savel'ev, A. L. Rakhmanov, and F. Nori, Phys. Rev. E **72**, 056136 (2005).
[19]O. G. Turutanov, V. I. Shnyrkov, M. Glukhov, Fiz. Nizk. Temp. **34**, 37 (2008) [Low Temp. Phys. 34, 37 (2008)].
[20]V. I. Shnyrkov, A. A. Soroka, and O. G. Turutanov, Phys. Rev. B **85**, 224512 (2012).
[21]A. Barone and G. Paterno, *Physics and Applications of the Josephson Effect* (Wiley, New York, 1982).
[22]A. M. Korolev, V. M. Shulga, O. G. Turutanov, V. I. Shnyrkov, Pribory i Tekhnika Eksperimenta 4, **37** (2015) [Instrum. Exp. Tech. **58**, 478 (2015)].
[23]O. G. Turutanov, V. Y. Lyakhno, and V. I. Shnyrkov, arXiv.org:1506.00953.
[24]V. A. Khlus, Fiz. Nizk. Temp. **12**, 25 (1986) [Sov. J. Low Temp. Phys. 12, 14 (1986)].

Translated by AIP Author Services.